Materials Science and Engineering C 70 (2017) 535–543

Contents lists available at ScienceDirect

Materials Science and Engineering C

journal homepage: www.elsevier.com/locate/msec

Polydiacetylene/triblock copolymer nanosensor for the detection of native and free bovine serum albumin

Jaqueline de Paula Rezende [a], Guilherme Max Dias Ferreira [b], Gabriel Max Dias Ferreira [b], Luis Henrique Mendes da Silva [b], Maria do Carmo Hepanhol da Silva [b], Maximiliano Soares Pinto [c], Ana Clarissa dos Santos Pires [a,*]

[a] Department of Food Technology, Universidade Federal de Viçosa, Av, PH Rolfs, s/n, Campus Universitário, Viçosa, MG 36570-000, Brazil
[b] Department of Chemistry, Universidade Federal de Viçosa, Av, PH Rolfs, s/n, Campus Universitário, Viçosa, MG 36570-000, Brazil
[c] Institute of Agrarian Sciences, Universidade Federal de Minas Gerais, Av. Universitária, 1000, Bairro Universitário, Montes Claros, MG 39404-547, Brazil

ARTICLE INFO

Article history:
Received 6 May 2016
Received in revised form 18 August 2016
Accepted 6 September 2016
Available online 7 September 2016

Keywords:
Nanosensor
Milk protein
Fluorescence
Microcalorimetry
Zeta potential

ABSTRACT

Bovine serum albumin (BSA) has been recognized as a marker of the cow's health, milk quality, an allergenic protein and as a carrier. Its detection is important in the food, pharmaceutical and medical industries. However, traditional techniques used to detect BSA are often time-consuming, expensive, and show limited sensitivity. This paper describes properties of polydiacetylene-triblock copolymer (L64) nanosensors, synthesized to easily detect BSA. Sensor efficiency was studied as a function of nanosensor composition, polydiacetylene chemical structures, BSA conformation and hydrophobic domain availability, using spectroscopic, calorimetric, light scattering, and electrokinetic analyses. Nanosensors were sensitive to detect the average BSA concentration of milk and dairy products and discriminated between native and denatured protein through naked-eye detectable blue-to-red transition. The standard Gibbs free energy ($-10.44 < \Delta G° < -49.52$ kJ M), stoichiometry complex ($1 <$ "n" < 3), and binding constant ($6.7 \times 10^2 < K_a < 4.79 \times 10^8$ M^{-1}) of BSA-nanosensor complex formation established a direct relationship between nanosensor response and BSA-nanosensor interaction. BSA-nanosensor interaction was entropically (without cholesterol), and enthalpically driven (with cholesterol). Eugenol-BSA complex did not induce colorimetric transition. Polydiacetylene-L64 nanosensors are potential low-cost sensors for rapid detection of BSA, discriminating between native/denatured and free/bound protein.

1. Introduction

Bovine serum albumin (BSA) detection has attracted increasing attention [1,2] mainly due to the application of BSA in different fields such as food, biochemical and immunological sciences. BSA has been used as a marker of the health of the cow's mammary gland and milk quality [3], and has been recognized as a significant allergenic protein [4]. It is widely used as a protein calibrant [5], and it can be used as ligand-carrier in applications relevant to the food and pharmaceutical industry [6,7].

Traditional techniques used to detect BSA are often based on spectrometric methods [8,9]. However, these methods suffer limitations such as complicated steps, expensive equipment, limited sensitivity and narrow linear range, and commonly shortening of the detection time is required. Therefore, it is necessary to develop alternative ways to detect small amounts of BSA in different matrixes, in real-time. Recently, some sensitive techniques such as matrix-assisted laser desorption/ionization time-of-flight mass spectrometry (MALDI-TOF-MS) and laser desorption/ionization time-of-flight mass spectrometry (LDI-TOF-MS) have improved protein identification in biological samples [10,11]. Nanomaterials can also be combined with analytical chemistry to develop ultra-sensitive detection methods [12], and can also improve sensitivity of colorimetric sensors.

Polydiacetylenes (PDAs) are conjugated polymers with the unique intrinsic ability to respond to different stimuli, undergoing blue-to-red transition [13]. Using colorimetric changes, some systems based on PDAs have been constructed to detect bacteria [14], enzymes [15], viruses [16], surfactants [17], solvents [18], and others. These chromic properties makes PDA suitable for use in sensor systems, with several merits such as simple and rapid detection, easy recognition through naked eye color change, and label-free detection [16].

PDAs may exist in self-assembled form in different structures, such as liposomes or vesicles [19,20], films [21], and nanocomposites [17], based on the preparation method, and/or chemical nature of the molecules used in synthesis [22]. In addition, colorimetric transition in these sensor systems is dependent on PDA aggregation form [21,23].

* Corresponding author.
E-mail address: ana.pires@ufv.br (A.C.S. Pires).

http://dx.doi.org/10.1016/j.msec.2016.09.009
0928-4931/

The application of PDA vesicles in the detection of different molecules in suspension has been widely studied. However, they have been found to show some limitations, such as low stability for long periods [24], and restricted colorimetric transition for some conditions, that could make difficult the visual detection of color change. It would therefore be useful to develop new PDA-based templates for the efficient use of this polymer as a sensor to detect different molecules. Gou et al. [25] showed that PDAs are able to interact with amphiphilic molecules such as triblock copolymers (TCs). These molecules are formed by arrays of ethylene oxide and propylene oxide units (symbolized as $(EO)_n(PO)_m(EO)_n$, where "n" and "m" mean the number of ethylene oxide and propylene oxide unit segments, respectively) [26]. These polymers are able to form micelles, and the self-assembly of TC has been used to produce nanostructures for many applications [27,28].

Therefore, in this study, to overcome limitations of PDA vesicles, nanoaggregates formed by a mixture of two polymers (PDA and triblock copolymer L64) were used to detect BSA. Nevertheless, to develop efficient nanosensors for future application in food, biomedical and/or pharmaceutical areas is essential to understand the mechanisms of BSA-nanosensor interaction that leads to protein detection in different conditions. Thus, besides our attention in detecting the protein we were also interested in determining the thermodynamic parameters associated with nanosensor-protein interaction, and in investigating the effects of nanoaggregate composition, protein conformation, and presence of protein-ligand on the colorimetric transition of polydiacetilenic nanosensors.

2. Materials and methods

2.1. Materials

BSA (98% wt. pure), α-lactalbumin (85% wt. pure), β-lactoglobulin (90% wt. pure), lactoferrin (85% wt. pure), α_{S1}-casein (70% wt. pure), β-casein (98% wt. pure), 10,12-pentacosadiynoic acid (PCDA, 97% wt.), 10,12-tricosadiynoic acid (TCDA, 98% wt.), cholesterol (99% wt. pure), eugenol (99% wt. pure), sodium chloride (NaCl, 99.5% wt. pure), calcium chloride ($CaCl_2$, 96% wt. pure), potassium chloride (KCl, 99% wt. pure), sodium carbonate sodium chloride (Na_2CO_3, 99% wt. pure) and sodium phosphate sodium chloride (Na_3PO_4, 99% wt. pure) were purchased from Sigma-Aldrich (USA). Glucomacropeptide (80% wt. pure) was acquired from Davisco (USA). Poly(ethylene oxide)-poly(propylene oxide)-poly(ethylene oxide) TC L64 [$(EO)_{13}(PO)_{30}(EO)_{13}$], with average molar mass (M_m) of 2900 $g \cdot mol^{-1}$, acquired from Aldrich (USA), was used. Polyvinylidene difluoride (PVDF) syringe filters (0.33 mm of diameter and 0.45 μm pore) were purchased from Millipore (USA), and Millipore water, were used in all experiments ($R \geq 18.2\ M\Omega \cdot cm$).

2.2. Nanosensor production

Nanosensors of PCDA and L64 were prepared by solubilizing L64 in water, at concentration of 1.0% (w/w). PCDA (1 mM) was dissolved in this TC solution, the mixture was sonicated for 10 min (Sonics & Materials Inc., Model VC750, USA), and immediately filtrated through PVDF filter. The suspension was kept overnight at 4 °C, with the aim of orientating PCDA monomers in order to promote polymerization. Next, photopolymerization was carried out by exposing the suspension to UV radiation (254 nm), for 6 min, until the suspension turned blue in color.

To investigate the effects of diacetylene monomer, nanosensors containing TCDA (1 mM) instead of PCDA, and L64 1.0% (w/w) were synthesized following the same steps as described above.

To evaluate the effect of a lipid insertion on color transition caused by BSA, nanosensors containing cholesterol (CHO) were manufactured. CHO (1, 2 or 3 mM) was dissolved into L64 solution (1% wt.) and the mixture was sonicated for 5 min; then PCDA or TCDA (1 mM) was added and the synthesis followed as described above for nanosensors without CHO.

2.3. Colorimetric response (CR)

In order to study the interaction between BSA and PCDA/L64 or TCDA/L64 nanosensor, BSA solution (0.75 mM) was prepared by solubilizing the protein in L64 1% (wt.). This procedure aimed did not dilute nanosensors suspension, maintaining L64 concentration constant. Aliquots of BSA solution were added to the nanosensor suspension, at increasing concentrations up to a final concentration of 0.20 mM. The mixtures were stirred for 30 s, and maintained at 25 °C for 1 h, to allow the system to achieve thermodynamic equilibrium. Spectra were obtained between 350 and 900 nm (Shimadzu UV-2550, Japan), at 25 °C. To quantify the percentage of blue-to-red conversion of polydiacetylenes, a parameter termed "colorimetric response (CR)" was calculated using Eq. 1 [29].

$$CR\ (\%) = \left(\frac{\left(\frac{A_{blue}}{A_{blue}+A_{red}}\right)_b - \left(\frac{A_{blue}}{A_{blue}+A_{red}}\right)_a}{\left(\frac{A_{blue}}{A_{blue}+A_{red}}\right)_b} \right) \times 100 \quad (1)$$

where A is the absorbance of blue (λ ~ 640 nm) and red components (λ ~ 540 nm), determined by UV–Vis spectroscopy. The terms "blue" and "red" are related to material appearance, and the indices "b" and "a" represent the absorbance before and after protein addition, respectively.

As we were interested in evaluating the effect of protein conformation, and bound protein on nanosensor CR, the procedures described above were repeated using the same concentration range, but changing BSA, denatured BSA, and eugenol-bound BSA, respectively.

In order to evaluate the stability of colorimetric nanosensors to pH change, the pH of suspensions was adjusted between 1.0 and 9.0 (at one-unit intervals) and CR was determined for each pH. We also evaluated the effect of interfering molecules (proteins, peptide and salts) on CR of nanosensors at concentration and double concentration that they are found in milk.

2.4. Light scattering and electrokinetic measurements

Size and zeta potential of nanostructures were measured at 25 °C, with a Zetasizer nano ZS90 (Malvern, UK). Samples were diluted 20 times to avoid blue color interference on the measurements. Each experiment was repeated 3 times, and each result was presented as the average of 10 measurements.

2.5. Fluorescence experiments

Fluorescence spectra of protein were recorded in a CaryEclipse Fluorescence Spectrometer (Agilent, USA), using a 1/cm path length quartz cuvette. Nanosensor aliquots were added to the protein (BSA or denatured-BSA) solution (0.75 mM), and the fluorescence emission spectra were recorded between 296 and 500 nm, at the excitation wavelength of 295 nm, which is specific for tryptophan residue excitation.

2.6. Isothermal titration microcalorimetric (ITμC) experiments

Titration analyses were performed in an isothermal titration microcalorimeter (ITμC), model CSC 4200 (TA Instruments Inc., USA), controlled by ITCRun software. The microreaction system (1.8-mL stainless steel vessels for sample and reference), containing PCDA/L64 or TCDA/L64 nanosensors, was maintained under constant stirring at 300 rpm, and analyzed in titration mode. When thermal equilibrium between the vessel and the heat sink was reached, 10-μL aliquots of protein (BSA, denatured-BSA or eugenol-bound BSA) solution were

titrated with a Hamilton microliter syringe at 500 s intervals, until protein concentration of 0.20 mM was achieved.

For each injection, the experimental enthalpy change (ΔH) was obtained by raw data peak integration. The values of integrated molar enthalpy change were obtained by dividing "ΔH" by the number of moles of BSA added in each injection ($\Delta_{Obs}H$). A control experiment was carried out in each run to determine the dilution enthalpy change ($\Delta_{dil}H$), by injecting BSA solution into nanosensor solvent (copolymer L64).

As the amount of BSA molecules bound per PCDA was not known, it was not possible to calculate the exact molar enthalpy change of interaction. Therefore, an apparent enthalpy change of interaction ($\Delta_{ap\text{-}int}H$) was determined, calculated from the difference between $\Delta_{Obs}H$ and $\Delta_{dil}H$ curves.

All calorimetric measurements were performed in triplicate, and the calculated relative standard deviation in the interaction enthalpy was found to be of the order of 0.5%.

2.7. Detection of BSA in milk sample

In order to evaluate the performance of nanosensors for detecting BSA in a real system, samples ($n = 10$) of skimmed milk were used. Milk was centrifuged at 25,000 *g* for 30 min at 20 °C for five times to remove casein micelles [30], eliminating the sample turbidity and the interference of casein micelle on nanosensor's response [31]. Aliquots (100 μL) of supernatant previously diluted 25 times in water, was added into 1 mL of PCDA/L64/CHO 1 mM suspension. The mixture was stirred for 30 s, maintained at 25 °C for 1 h, then spectra were obtained between 350 and 900 nm, and the CR was obtained by Eq. 1. In order to evaluate the potential of PCDA/L64/CHO 1 mM as a sensor for quantifying BSA in milk, we also performed BSA analysis using reversed-phase high performance liquid chromatography (RP-HPLC) model AKTAExplorer (GE Healthcare Life Sciences, Sweden), according to Billakanti et al. [32].

3. Results

3.1. Optical properties, size and electrokinetics potential of polydiacetylenic/L64 nanostructures

Diacetylene self-organized and irradiated at 280 nm polymerize producing "blue" macromolecule. The presence of either copolymer or CHO did not inhibit diacetylene polymerization, and the electronic spectra of all nanosensors were found to present similar profiles, with maximum absorption band at 640 nm, and a shoulder at 590 nm (Fig. 1). However, the intensity of both bands increased with CHO concentration, showing that the presence of lipid increased the polymerization yield.

CHO also affected nanosensor hydrodynamic diameter (D_h), and zeta potential (ξ) ($p < 0.05$). Nanosensors without CHO presented D_h and ξ equal to 78.20 ± 1.39 nm and −22.20 ± 0.12 mV, respectively. The addition of CHO resulted in the nanostructure being smaller (65.80 ± 0.94, 62.90 ± 1.28 and 67.40 ± 1.40 nm), and more negatively charged (−29.50 ± 0.66, −29.50 ± 0.58 and −28.30 ± 0.75 mV) ($p < 0.05$), for CHO concentrations equal to 1, 2, and 3 mM, respectively, which did not change between them ($p \geq 0.05$).

3.2. Polydiacetylene nanostructure interaction with BSA resulting in an optical nanosensor for BSA

Before investigate the efficiency of colorimetric nanosensors for detecting BSA, it is important to determine the stability of the nanostructures against pH and presence of interfering molecules. Between pH 4.0 and 9.0 there was no change in color, D_h and ξ parameters for all nanostructures; however below pH 4.0 systems precipitated due to the reduction of electrostatic repulsion between carboxylic groups at nanosensor interface. In addition, above pH 9.0, there was color transition, and thus systems in these conditions could not be used as sensors. Since there was no difference between the different nanostructures for pH response ($p \geq 0.05$), the CR, Dh and ξ averages of all nanosensors as a function of pH change are presented in Fig. S1 (Supplementary Materials).

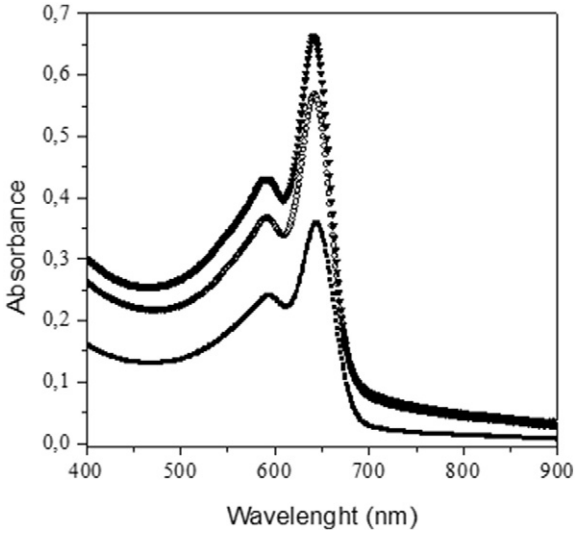

Fig. 1. UV–vis spectra of PCDA/L64 nanoblends, containing: (■) 0 mM, (○) 1 mM, and (▼) 3 mM cholesterol.

The presence of most of tested salts (NaCl, KCl, $CaCl_2$ and Na_2CO_3) did not change the color of nanosensors; however Na_3PO_4 was able to convert PCDA from the blue to the red form (CR ~ 80%) (Fig. S2, Supplementary Materials). In a previous work, our group showed that phosphate ions released from casein micelle acted as a stimuli promoting colorimetric transition of PCDA nanostructure [31].

To evaluate the effect of milk proteins or peptide on colorimetric transition of PCDA/L64 nanosensors, increasing concentrations of BSA, or α-lactalbumin or β-lactoglobulin or lactoferrin or α_{S1}-casein or β-casein or glucomacropeptide was added into nanosensor suspension. Blue-to-red transition of nanosensors only occurred in the presence of BSA. The extension of PCDA conversion due to interaction with BSA was determined using the colorimetric response (CR) parameter. Fig. 2a illustrates the CR of different PCDA/L64 1.0% (w/w) nanosensors as a function of BSA concentration at 25 °C. Fig. 2b shows the small effect of other proteins (α-lactalbumin or β-lactoglobulin or lactoferrin or α_{S1}-casein or β-casein) and glucomacropeptide on optical properties of nanosensors (CR < 5%). Results are expressed as CR average because there is no difference ($p \geq 0.05$) between nanosensors with or without CHO.

CR was enhanced as BSA concentration increased, achieving a plateau of maximum CR at BSA concentration of 0.18 mM, with maximum CR of 34%, 65%, 60%, and 43% for PDA/L64 nanosensor containing 0, 1, 2, and 3 mM cholesterol, respectively. It was verified color change by naked eye for only PCDA/L64/CHO 1 mM and PCDA/L64/CHO 2 mM nanosensors (Fig. S3, Supplementary materials). As PCDA/L64/CHO 1 mM showed a slightly higher CR, we calculated the limit of detection (LOD) for BSA of this nanosensor through a calibration graph (Fig. S4 at Supplementary materials). LOD was 0.05 mM BSA, which covers BSA concentration present in milk and dairy products. Other techniques can detect smaller amount of BSA (in nanomolar scale), as such as labelling fluorescence spectroscopy [2,9,33], MALDI-TOF-MS [10] and LDI-TOF-MS [11], however for dairy systems PCDA/L64/CHO 1 mM seems to be simple and fast nanodevice to detect BSA.

Thermochromism experiments carried out using all nanoaggregates showed that on increasing CHO concentration, the rotational barrier energy (ΔE_{RB}) values increased slightly (since higher temperatures induced the colorimetric transition, see Fig. S5 in Supplementary materials).

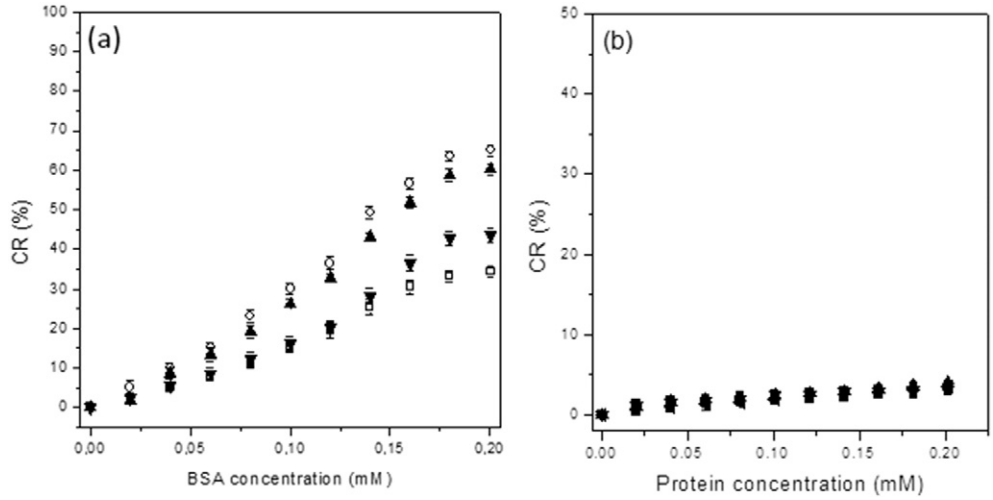

Fig. 2. (a) Colorimetric response (CR, %) of nanoblends formed by PCDA (1 mM) and L64 1% (w/w), containing cholesterol at concentration (□) 0 mM, (○) 1 mM, (▲) 2 mM and (▼) 3 mM, as a function of BSA concentration, at 25 °C; and (b) CR average (%) of nanoblends formed by PCDA with and without cholesterol as a function of (□) α-lactalbumin, (○) β-lactoglobulin, (▲) lactoferrin, (▼) α_{S1}-casein, (■) β-casein and (◄) GMP concentration, at 25 °C.

The addition of BSA to nanosensor aqueous suspension reduced the nanosensor diameter. Nanosensors with higher CR (containing 1 and 2 mM CHO) reduced by around 50% of their diameter, while the others reduced by only 30% (Fig. 3a), probably due to increased polydiacetylene conversion from blue to red form, by linear-coil transition altering molecular packing degree [34].

Zeta potential of nanosensor systems was also obtained. To ensure that ξ values were related to nanosensors (and not to BSA) we measured the zeta potential of BSA in the L64 solution, and found it to be -13.2 ± 0.4 mV. All nanosensors were found to be negatively charged, with a decrease in their zeta potential (from −22.0 to −29.0 mV) in the presence of CHO, demonstrating that the ξ values measured were clearly related to nanosensors. As BSA was added to nanosensor suspension, ξ became less negative (Fig. 3b).

The BSA fluorescence intensity reduced and there was a displacement in the maximum peak (around 5 nm) as PCDA concentration increased (Fig. S6, Supplementary materials), indicating BSA-PCDA complex formation. To determine BSA-nanosensor binding constant (K_a), we followed Stern-Volmer approach using Eq. 2.

$$log\frac{(F_0-F)}{F} = logK_a + nlog[PCDA] \quad (2)$$

where "F_0" and "F" are the fluorescence intensities of BSA, in the absence and presence of quencher (in this case PCDA, since pure L64 micelle did not quench BSA fluorescence), respectively. K_a and "n" denote the binding constant for BSA-PCDA interaction, and the complex stoichiometry, respectively, calculated by linear regression of log [(F_0—F)/F] × log [PCDA] plots (Fig. S6, Supplementary materials).

Using Eq. 3, the ΔG° for complex formation was calculated. If ΔG° < 0, the equilibrium BSA + PCDA ↔ BSA-PCDA shifts to BSA-PCDA complex, while ΔG° > 0 favors the presence of reactants.

$$\Delta G^{\circ} = -RTlnK_a \quad (3)$$

where R is ideal gas constant (8.314 J mol^{-1} K^{-1}), T is absolute temperature (K) and K_a is binding constant. K_a, "n" and ΔG° values obtained for BSA interaction with the different nanosensors are found in Table 1.

K_a, "n" and ΔG° values depended on nanostructure composition, with the following order for their modulus: PCDA/L64 < PCDA/L64/CHO 3 mM < PCDA/L64/CHO 2 mM < PCDA/L64/CHO 1 mM.

To characterize the BSA-nanosensor complex formation process in detail, the enthalpic contribution for BSA-nanosensor interaction was determined by microcalorimetric assays. Fig. 4a shows the apparent interaction enthalpy change ($\Delta_{ap\text{-}int}H$) between BSA and PCDA/L64

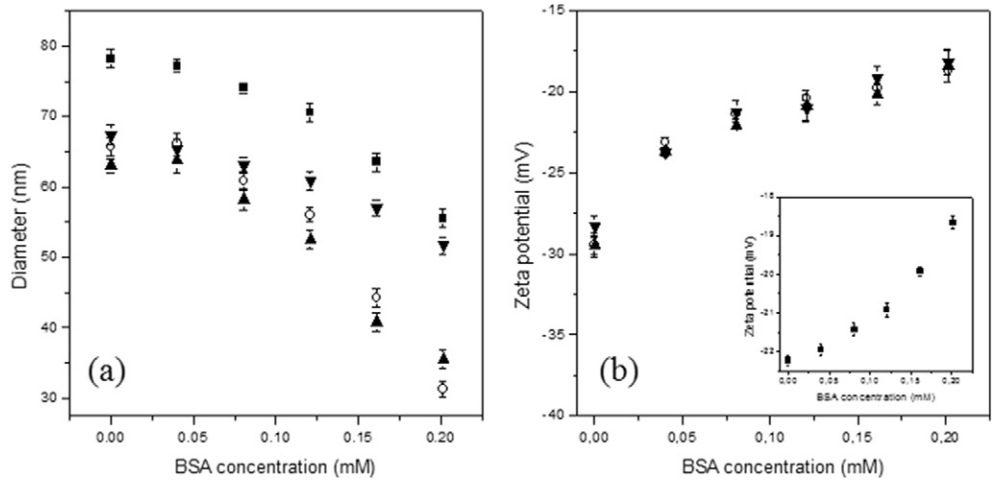

Fig. 3. Effect of BSA addition on (a) hydrodynamic diameter, and (b) zeta potential of nanoblends containing (■) 0 mM, (○) 1 mM, (▲) 2 mM and (▼) 3 mM cholesterol, as a function of BSA concentration, at 25 °C.

Table 1
Binding constant (K_a), complex stoichiometry (n), and standard free Gibbs energy change ($\Delta G°$) for BSA-PCDA complex formation, at 25 °C.

Nanoblend	K_a (10^8 L mol^{-1})	n	R^2	$\Delta G°$ (kJ mol^{-1})
PCDA/L64	0.22 ± 0.01	1.6	0.99	−30.52 ± 1.22
PCDA/L64/CHO 1 mM	4.79 ± 0.19	2.7	0.99	−49.52 ± 1.74
PCDA/L64/CHO 2 mM	1.35 ± 0.05	2.3	0.99	−40.68 ± 1.43
PCDA/L64/CHO 3 mM	0.69 ± 0.02	1.8	0.98	−33.31 ± 1.27

nanosensors, containing or not containing CHO, versus BSA concentration.

In the absence of CHO, interaction between BSA and the nanosensor was found to be an endothermic process, with $\Delta_{ap\text{-}int}H$ of 22.82 kJ·mol^{-1}, at a concentration of 9.11 μM BSA (first injection). At a protein concentration of 164.00 μM (PCDA/BSA ratio of 1.5), $\Delta_{ap\text{-}int}H$ became constant at almost zero, indicating the saturation of nanosensor sites.

On the other hand, at either CHO concentration (1 or 3 mM), the interaction process between BSA and nanosensor was exothermic, releasing −2.68 kJ·mol^{-1} (at 3 mM CHO) and −42.20 kJ·mol^{-1} (at 1 mM CHO), at 9.11 μM BSA (first injection). $\Delta_{ap\text{-}int}H$ values became less negative with an increase in BSA concentration, until a plateau was reached at BSA concentrations of 160.55 and 182.22 μM, for lipid concentration of 3.0 and 1.0 mM, respectively, again suggesting nanosensor saturation.

3.3. The effect of polydiacetylene chain length on nanosensors properties

To assay the effect of hydrophobic tail length of diacetylene monomers on ΔE_{RB} (consequently, on color transition of nanosensors), we replaced PCDA by 10,12-tricosadyinoic acid (TCDA), which has 2 fewer carbon atoms than PCDA. Fig. 5 illustrates the TCDA/L64 nanosensor CR as a function of BSA concentration, in the presence or absence of CHO.

The replacement of PCDA by TCDA monomers resulted in a remarkable increase in CR, even in the absence of CHO. The maximum CR was 93%, at 0.18 mM BSA, and in the presence of 1 mM CHO, CR was also greater for TCDA/L64 than for PCDA/L64 nanosensor.

In order to understand the molecular basis of the difference between BSA-TCDA/L64 and BSA-PCDA/L64 nanosensor interaction, fluorescence and microcalorimetric experiments were also carried out. For fluorescence analysis, similar to that observed for PCDA/L64 nanosensors, there was a displacement (6 nm) in the wavelength of the maximum peak of BSA emission spectra. Using Stern-Volmer approach, by Log [(F_0—F)/F] × Log [TCDA] plots, K_a and "n" were obtained, and ΔG° was calculated from Eq. 3 (see Fig. S7 and Table S1 in Supplementary materials).

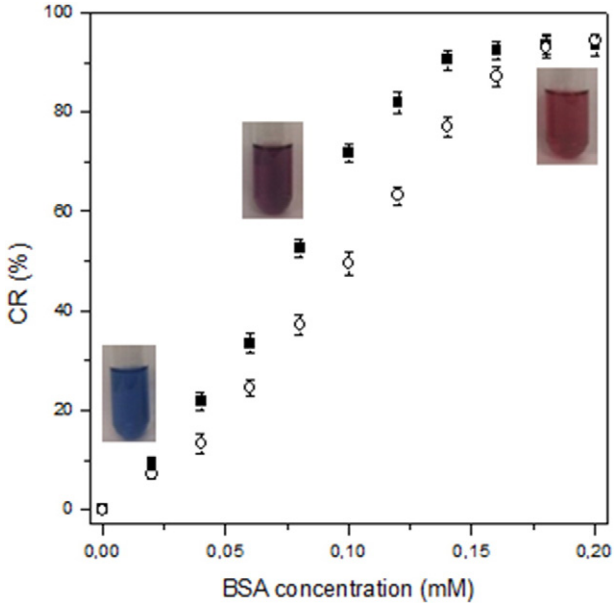

Fig. 5. Colorimetric response (CR, %) of nanoblends formed by TCDA (1 mM) and L64 1% (w/w) at (■) 0 mM and (○) 1 mM cholesterol, as a function of BSA concentration, at 25 °C. Pictures correspond to naked-eye color detection in each curve region.

As observed for PCDA nanosensors, more negative ΔG° values for BSA-TCDA nanosensor interaction resulted in more sensitive TCDA nanosensors (TCDA/L64/CHO 1 mM > TCDA/L64). Despite the higher sensitivity of TCDA nanosensors compared to PCDA ones, the BSA-TCDA interaction energy and complex stoichiometry were found to be lower than those obtained for the BSA-PCDA complex.

Microcalorimetric data for BSA-PCDA/L64 and BSA-TCDA/L64 nanosensor interactions were similar for nanostructures without CHO, in all BSA concentrations studied. On the other hand, for nanosensors with 1 mM lipid, the $\Delta_{ap\text{-}int}H \times$ [BSA] curve for BSA-PCDA/L64 was exothermic (Fig. 4a); while for BSA-TCDA/L64 it was endothermic (Fig. 4b).

Despite the higher colorimetric sensitivity of TCDA/L64 nanosensors for detection of BSA, these nanosensors show less stability than PCDA/L64 nanostructures during storage. Therefore, we chose to continue

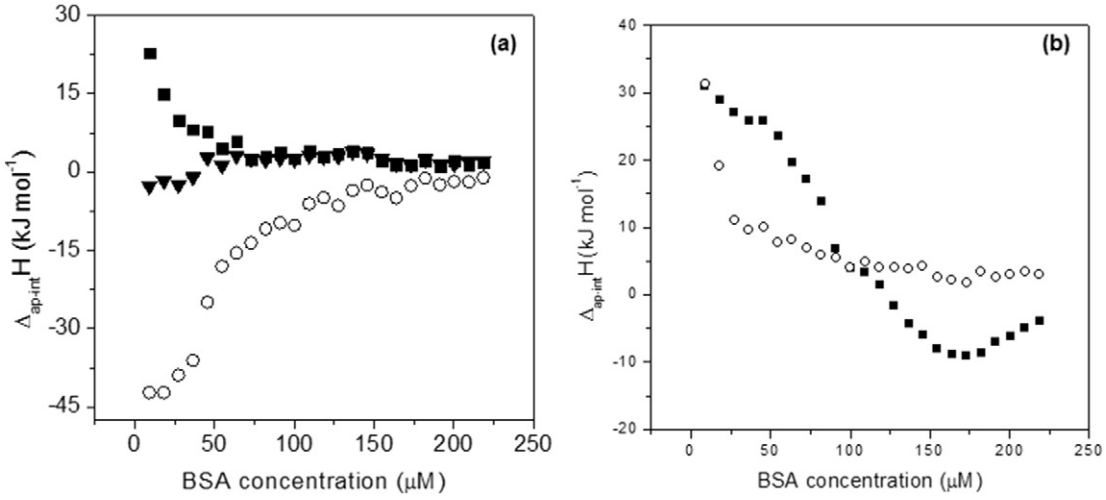

Fig. 4. $\Delta_{ap\text{-}int}H$ versus BSA concentration between (a) BSA and PCDA/L64 nanoblends containing (■) 0 mM, (○) 1 mM, and (▼) 3 mM cholesterol, and (b) BSA and TCDA/L64 nanoblends containing (■) 0 mM and (○) 1 mM cholesterol, at 25 °C.

this investigation using more stable nanosensors (PCDA/L64 nanosensors).

3.4. Effect of the three-dimensional structure of biopolymer on the BSA-nanosensor interaction

To evaluate the effect of protein conformation change on BSA-nanosensor interaction, we performed all previous experiments again, with denatured BSA and nanosensors PCDA/L64 and PCDA/L64/CHO 1 mM. Fig. 6a shows the CR of PCDA as a function of denatured-BSA concentration.

The maximum CR for both nanosensors in the presence of denatured BSA achieved only 5%, demonstrating that biopolymer conformation is found to play an important role in BSA-PCDA and/or BSA-CHO interactions.

Fluorimetric and microcalorimetric experiments confirmed the small interaction between denatured BSA and nanosensors, since there was no fluorescence quenching process, and enthalpy change measurement indicated very small energy values (Fig. S8a and S8b, Supplementary materials).

3.5. Effect of eugenol-BSA complex formation on interaction between protein and nanosensors

The presence of eugenol entrapped within the protein molecule decreased nanosensor CR (Fig. 6b). The maximum CR values were reduced from 34% (free-BSA) to 14% (eugenol-BSA complex), and from 65% (free-BSA) to 5% (eugenol-BSA complex), for PCDA/L64 and PCDA/L64/CHO 1 mM, respectively, demonstrating the importance of hydrophobic region for BSA-nanosensor interaction.

Microcalorimetric measurements showed that eugenol-BSA complex interaction with both nanosensors was found to be endothermic and weak, with $\Delta_{ap\text{-}int}H$ values almost constant, and around 1 and 3 kJ mol^{-1} for PCDA/L64 and PCDA/L64/CHO 1 mM respectively, at all BSA concentrations (See Fig. S9 in Supplementary materials).

3.6. Detection of BSA present in milk sample

Milk is a complex matrix and many constituents may interfere in response of colorimetric nanosensors. Even these constituents separated did not show ability to convert PCDA from blue to red form, the interactions present in milk may change this result. Thus, the performance of PCDA/L64/CHO 1 mM for detecting BSA was tested for milk samples. The nanosensors containing 100 μL of diluted skimmed milk underwent visible blue-to-red transition, and the CR average for samples was 50 ± 2.5%, indicating that diluted samples had around 0.180 mM of BSA. Correcting this value using dilution factor (25), our nanosensor found that milk samples had 0.450 ± 0.03 mM BSA, while RP-HPLC analysis detected 0.425 ± 0.02 mM; however using student *t*-test with 95% confidence interval, there was no difference ($p \geq 0.05$) between our nanosensor and RP-HPLC technique (Fig. S10, Supplementary materials).

4. Discussion

Triblock copolymers molecules poly(ethylene oxide)-poly(propylene oxide)-poly(ethylene oxide) (PEO-PPO-PEO) can self-assemble in micelles, depending on temperature and concentration. They can form a hydrophobic core of PPO segments able to solubilize diacetylene monomers. Since L64 critical micellar concentration (c.m.c) is 0.35% (w/w) at 25 °C [35], mixtures of copolymer aqueous solution (1.0%, w/w) and PCDA monomers produced aggregates containing a hydrophobic core composed of PO segments and the hydrophobic tails of the PCDA monomers. At the hydrophobic/hydrophilic aggregate interface, the PCDA carboxylic groups are orientated towards the hydrophilic shell formed by the EO segments.

Due to specific interactions between CHO and BSA [36], we believed that lipid addition to the PCDA/L64 nanostructure may increase the nanosensor's efficiency for detecting this protein. The CHO added to the PCDA/copolymer mixture could be dissolved in the hydrophobic region, and/or at interface of the nanosensor, interacting with PO segments and PCDA monomers. As the PCDA polymerization process is dependent on the orientated packaging of PCDA monomers, the increase in absorption intensity indicates that CHO improved PCDA self-aggregation. The reduction in size and the increasing (in modulus) in zeta potential of nanoaggregates containing CHO corroborates with this hypothesis that CHO molecules are located at hydrophobic/hydrophilic interface and in the hydrophobic core of nanosensors.

It has been recognized that PCDA nanostructures are able to change their color from blue to red in the presence of proteins, indicating the occurrence of intermolecular interactions between them [31]. This PCDA color change could be due to the energy of the polydiacetylene molecules overcoming the rotational barrier energy (ΔE_{RB}), and changing their conformation from linear (blue) to random coil (red) form. At 1 and 2 mM, the presence of CHO improved the sensitivity of PCDA nanosensor for BSA detection, suggesting a specific interaction between

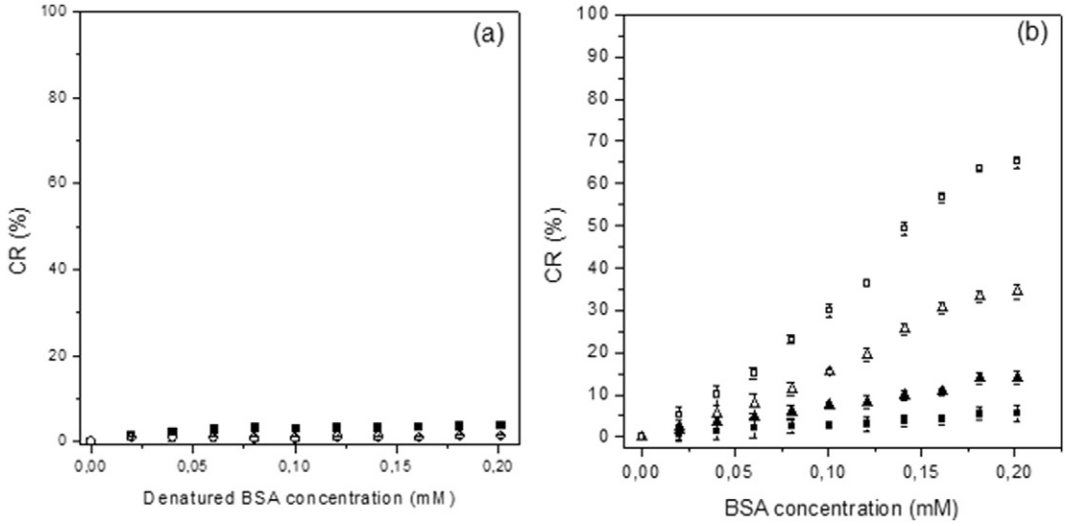

Fig. 6. (a) Colorimetric response (CR, %) of nanoblends formed by PCDA (1 mM) and L64 1% (w/w) containing cholesterol (■) 0 mM and (○) 1 mM, as a function of denatured-BSA concentration, (b) CR (%) of nanoblends formed by PCDA (1 mM) and L64 1% (w/w) (Δ, ▲) 0 mM and (□, ■) 1 mM cholesterol, as a function of eugenol-BSA complex concentration, at 25 °C. Open symbols represent free-BSA and filled symbols represent BSA bound to eugenol.

the protein and lipid, and/or intermolecular interactions between PCDA and CHO, decreasing the PCDA ΔE_{RB}. Nevertheless, CR reduced when CHO concentration increased to 3 mM, which may be related to PCDA stabilization (enhancing ΔE_{RB}), caused by CHO concentration increasing, since it is known that at higher CHO concentration the lipid segregation process may limit the conformational freedom of PCDA [37]. Thermochromism data demonstrated that the higher sensitivity of PCDA/L64/CHO 1 mM should not be attributed to decreasing ΔE_{RB}. Therefore, this higher sensitivity seems to occur due to specific BSA-CHO interactions at the BSA-PCDA/L64/CHO 1 mM complex interface, as demonstrated by Charbonneau et al. [36]. However, for higher CHO concentration (3 mM), lipid molecules could be segregated in pure nano-domains, increasing the CHO-CHO interaction to the extent that BSA-CHO interaction was avoided. Bukiya et al. [38] demonstrated this same phenomenon, termed "cholesterol condensation effect" in liposomes.

As L64 concentration in nanosensor aqueous suspension is above c.m.c., the occurrence of L64 micelle formation, with size of approximately 10 nm at 25 °C, is possible [39]. However, the size of nanosensor aggregate was between 62 and 78 nm (Fig. 3a), which demonstrates that its structure is higher than L64 micelles. The increasing CHO concentration decreased the hydrodynamic diameter (D_h) of nanoaggregates, pointing to a higher packaging degree of molecules, and/or a lower aggregation number in the presence of the lipid, possibly due to a preferential interaction between CHO and polydiacetylene molecules, and/or CHO and propylene oxide segments. It is known that CHO interacts with lipids and hydrophobic molecules by hydrophobic interactions [40,41].

As this lipid is not ionized at the pH of nanosensor aqueous suspension (pH 8.5) due to the pKa of hydroxyl group of CHO being around 15 [42], the effect of CHO on the surface charge of nanoaggregate is due to CHO-PCDA interactions (mainly hydrogen bonding), which promote changes in the degree of ionization of carboxylic groups at the nanosensor interface. This effect was not found to be dependent on CHO concentration, possibly because at above 1 mM CHO, the nanosensor interface is saturated and lipid molecules diffuse inside the nanoaggregate forming nano-domains, intensifying CHO-CHO interaction. However, the interaction between BSA and PCDA/L64 nanosensor neutralized some of the negative charge at the nanoaggregate interface. Despite the overall charge of BSA being negative, some protein amino acid residues are positively charged, allowing a direct electrostatic interaction between these and the negatively charged carboxylic groups of PCDA.

Since PCDA and L64 formed a nanoaggregate without phase segregation, as it has been verified for other triblock copolymers [43–45], we could consider it a nanoparticle, and thus measure binding parameters between BSA-nanoaggregate interaction. Fluorescence spectroscopy is a powerful technique to study the intermolecular interaction between BSA and PCDA/L64 nanosensors. BSA fluorescence results from 2 tryptophan residues, which when excited at 295 nm emit electromagnetic radiation at a wavelength range of between 320 and 370 nm. By measuring the fluorescence quenching of the biopolymer when protein-nanosensor complexes are formed, thermodynamic parameters were determined and help us to understand the driven forces on BSA-nanoaggregate interactions and, consequently, on BSA detection. The more intense the BSA-nanoaggregate interaction (lower $\Delta G°$ values), and the greater the number of PCDA molecules per protein (higher "n"), the more sensitive the nanosensor. The magnitude of $\Delta G°$ values shows that BSA-nanosensor interactions should occur through dispersive interactions (van der Waals and London forces), electrostatic forces, and hydrogen bonding between PCDA carboxylic groups present at the nanosensor hydrophobic/hydrophilic interface and amino and carboxyl groups of BSA amino acid residues.

Microcalorimetric measurements were carried out in expectation of determining thermodynamic binding parameters for BSA and PCDA, however our calorimetric data did not adjust to the binding model because the product "Ka × [polydiacetylene]" was not between 50 and 500 [46]. Despite of this, the calorimetric measurements allowed us to gain important information about the forces that leaded BSA to interact with nanoblends (in the presence or in the absence of CHO). The $\Delta_{ap\text{-}int}H$ decreased as BSA concentration increased, showing that an increase in protein content decreased the number of nanosensor free interaction sites. The calorimetric saturation was close to CR saturation point (180 μM), demonstrating that when nanosensor sites were saturated, colorimetric transition reached its maximum value. The more intense $\Delta_{ap\text{-}int}H$ occurred at BSA concentrations between 0 and 75 μM, which in the CR curve correspond to BSA concentrations that induced only 10% of blue to red conversion. To understand this relatively small effect of PCDA colorimetric transition on $\Delta_{ap\text{-}int}H$ values, we must consider that $\Delta_{ap\text{-}int}H$ values are influenced by six molecular processes, including enthalpic change due to desolvation of PCDA ($\Delta_{des\text{-}PCDA}H$) and BSA ($\Delta_{des\text{-}BSA}H$) surfaces, interaction between PCDA and BSA ($\Delta_{PCDA\text{-}BSA}H$), PCDA conformational change ($\Delta_{conf}H$), reduction in PCDA ionization degree ($\Delta_{ion}H$), and change in nanostructure size ($+\Delta_{size}H$ for decrease, and $-\Delta_{size}H$ for increase, in nanosensor size), as shown in Eq. 4.

$$\Delta_{ap-int}H = \Delta_{des-PCDA}H + \Delta_{des-BSA}H + \Delta_{PCDA-BSA}H + \Delta_{conf}H + \Delta_{ion}H + \Delta_{size}H \quad (4)$$

As shown in Fig. 2a, 3a and b, at a BSA concentration range of between 0 and 75 μM, there was a small change in the parameters: CR, nanostructure size and ionization degree. Therefore, the enthalpic parameters $\Delta_{conf}H$, $\Delta_{size}H$, and $\Delta_{ion}H$ contributed only slightly to the magnitude of $\Delta_{ap\text{-}int}H$, showing that the main contributors to its value were the energies from PCDA and BSA desolvation ($\Delta_{des\text{-}PCDA}H$, $\Delta_{des\text{-}BSA}H$, respectively), and PCDA-BSA interaction ($\Delta_{PCDA\text{-}BSA}H$). As $\Delta_{ap\text{-}int}H$ values were found to be always positive, the energetic cost for desolvating PCDA and BSA molecules was higher than the energy released when both molecules interacted, indicating that the BSA-nanosensor interaction is entropically driven, due to the increase in mixture configurational entropy caused by BSA and nanosensor desolvating, with water release.

From 75 μM BSA until saturation point, there was a pronounced change in CR, size, and zeta potential of nanosensors, showing that the $\Delta_{conf}H$, $\Delta_{size}H$ and $\Delta_{ion}H$ parameters make an important contribution to $\Delta_{ap\text{-}int}H$ values. Therefore, the very small values for $\Delta_{ap\text{-}int}H$ were probably due to the compensation between positive ($\Delta_{conf}H$, $\Delta_{ion}H$, $\Delta_{des\text{-}PCDA}H$, $\Delta_{des\text{-}BSA}H$, and $\Delta_{size}H$) and negative ($\Delta_{PCDA\text{-}BSA}H$) parameters, according to Eq. 4.

As discussed above, the $\Delta_{ap\text{-}int}H$ values obtained in the case of BSA interaction with nanosensor containing lipid (1 and 3 mM CHO) resulted from the same molecular processes as described in Eq. 4, with four more terms added to show the following enthalpic changes: BSA-CHO ($\Delta_{BSA\text{-}CHO}H$), CHO-CHO ($\Delta_{CHO\text{-}CHO}H$), CHO-PCDA ($\Delta_{CHO\text{-}PCDA}H$), and CHO-copolymer ($\Delta_{CHO\text{-}L64}H$) interactions.

BSA-nanosensor interaction depended on the nanosensor CHO concentration resulting in, at small BSA concentration, $\Delta_{ap\text{-}int}H$ being much more negative for 1 mM, than for 3 mM lipid. The more exothermic process of BSA-nanosensor (1 mM CHO) interaction may be attributed to an intense and specific interaction between CHO and BSA that releases more energy than is absorbed to break CHO-PCDA, CHO-L64, and CHO-CHO interactions. On the other hand, for the BSA-nanosensor (3 mM CHO) interaction, less energy was released, possibly due to a segregation process involving CHO molecules forming nano-domains of pure lipids inside the nanosensor [38], which demands a higher energy cost to break CHO-CHO interaction that is released by BSA-CHO bonds.

For both nanosensors, at different lipid concentrations, as BSA concentration increases, $\Delta_{ap\text{-}int}H$ becomes less negative. This result occurs because the BSA binding in nanosensor promotes a change in nanostructure size, ionization degree and PCDA macromolecule conformation transition (blue-to-red colorimetric change). These nanosensor structural changes expend energy, causing an increasing in $\Delta_{ap\text{-}int}H$

values. For nanosensor (1 mM CHO), the $\Delta_{ap\text{-}int}H$ versus BSA concentration curve showed a higher slope, than for the same curve for nanosensor (3 mM CHO). As the ionization degree change for both nanosensors was similar, the $\partial \frac{\Delta_{ap-intH}}{\partial[BSA]}$ difference between 1 mM and 3 mM CHO curves may be attributed to the energy cost of nanostructure size and PCDA conformational change, which was more intense for nanosensor (1 mM CHO).

ΔE_{RB}, which modulates sensor sensitivity for color transition of polydiacetylenes, is determined by intermolecular interactions occurring between the hydrophobic tails of polydiacetylenes and copolymer segments, CHO, and other polydiacetylene chains. All of these interactions are dependent on polydiacetylene chain size. The maximum CR was reached at 0.18 mM for both nanosensors, indicating that the maximum number of sites for BSA interaction at the nanosensor interface was equal for PCDA and TCDA nanostructures. This higher sensitivity of TCDA nanosensors resulted from a rotational barrier reduction due to a decrease in the following interactions: TCDA-TCDA, TCDA-L64 and TCDA-CHO, associated with small diacetylene hydrophobic tails, and not from a more intense interaction between this nanosensor and BSA.

As the TCDA interaction with nanosensor components is less intense than the PCDA interaction with copolymer, CHO and other PCDAs, the molecular packing density is lower in TCDA nanostructure, resulting in CHO entrapment inside the nanosensor hydrophobic core. Therefore, CHO molecules are not available to interact with BSA, because of which this interaction makes no exothermic contribution to $\Delta_{ap\text{-}int}H$ values.

Protein conformation may also influence interaction with nanosensor components [47]. Probably, denaturation results in the exposure of many hydrophobic amino acid residues in an aqueous micro-environment, which creates a repulsive interaction between the BSA hydrophobic group and the hydrophilic segments of the poly (ethylene oxide) shell, mainly by exclusion volumetric mechanism [48]. This lack of blue-to-red transition of nanosensors in the presence of denatured protein makes it a useful nanosensor for discriminating native from denatured BSA molecules, thus providing an important analytical tool for application in many fields (e.g. food, pharmaceutical and health care) in which BSA is used.

The effect of the availability of BSA hydrophobic sites (free or occupied by another molecule) to interact with nanosensors was also studied. We believe that the hydrophobic sites of BSA (present in native BSA) may also play an important role in protein interaction with nanosensors and detection by them. Thus, we bound BSA with eugenol, a poor water soluble molecule that interacts with protein by entrapment into a hydrophobic domain of the biopolymer [49]. The CR of nanosensor reduced more in the presence than in the absence of CHO, corroborating with the previous suggestion that a specific interaction between BSA and CHO occurs. Thus, protein-lipid complex did not form in the presence eugenol-BSA complex due to the occupation of the protein hydrophobic domain. Microcalorimetric results confirm that when BSA interacts with eugenol, the protein hydrophobic site is unavailable to interact with CHO and/or nanosensor sufficiently to promote colorimetric transition.

When PCDA/L64/CHO 1 mM was tested to detect BSA in milk, a real sample, the nanosensor was able to detect the protein in the concentration range that it is commonly found in milk [50], using a diluted milk sample, as it was detected by RP-HPLC. It is important to emphasize that BSA detection using our nanosensor is cheaper, faster and simpler than chromatographic technique.

5. Conclusions

An optical nanosensor was synthesized by controlled self-assembly of polydiacetylene and copolymer molecules, and its efficiency of detection of BSA was demonstrated. The PCDA/L64 colorimetric transition was induced by a direct interaction between BSA and nanosensors, driven by an increase in entropy, when CHO was absent from the nanostructure composition, and driven by enthalpy in the presence of the lipid. A reduction in polydiacetylene hydrophobic tail length by only 2 carbon atoms was found to increase nanosensor sensitivity, mainly by diminishing the polydiacetylene rotational barrier energy. This nanosensor may be applied to determine the binding degree of BSA with hydrophobic compounds, since the eugenol-BSA complex was unable to induce nanosensor color transition. PCDA/L64 nanostructures showed efficient discrimination between denatured and native BSA, providing a very simple and low-cost analytical tool for ensuring conformational quality control of BSA samples. In addition, PCDA/L64/CHO 1 mM has potential as nanosensor for BSA detection in dairy samples.

Acknowledgements

The authors wish to thank CNPq (403119/2013-8 and 480344/2013-2) and FAPEMIG (APQ-01656-14 and APQ-02094-15) for their financial support, and J.P.R, G.M.D.F. and G.M.D.F. would like to thank CNPq and CAPES for providing a scholarship for this study.

Appendix A. Supplementary data

Supplementary data to this article can be found online at http://dx.doi.org/10.1016/j.msec.2016.09.009.

References

[1] E. Babu, P. Muthu, S. Singaravadivel, A selective, long-lived deep-red emissive ruthenium (II) polypyridine complexes for the detection of BSA, Spectrochim. Acta - Part A Mol. Biomol. Spectrosc. 130 (2014) 553–560, http://dx.doi.org/10.1016/j.saa.2014.04.060.
[2] X. Chen, Y. Xiang, A. Tong, Facile, sensitive and selective fluorescence turn-on detection of HSA/BSA in aqueous solution utilizing 2,4-dihydroxyl-3-iodo salicylaldehyde azine, Talanta 80 (2010) 1952–1958, http://dx.doi.org/10.1016/j.talanta.2009.10.053.
[3] A. Jantz, B. Finke, An improved analytical approach for the determination of bovine serum albumin in milk, Lait 85 (2005) 237–248, http://dx.doi.org/10.1051/lait.
[4] H.E. Indyk, B.D. Gill, D.C. Woollard, An optical biosensor-based immunoassay for the determination of bovine serum albumin in milk and milk products, Int. Dairy J. 47 (2015) 72–78, http://dx.doi.org/10.1016/j.idairyj.2015.02.011.
[5] Z. Liu, J.S. Gonzalez, H. Wang, S. Gunasekaran, T. Runge, Analytical methods dairy manure protein analysis using UV–Vis based on the Bradford method, Anal. Methods 7 (2015) 2645–2652, http://dx.doi.org/10.1039/C4AY03006K.
[6] A. Basu, G.S. Kumar, Thermodynamics of the interaction of the food additive tartrazine with serum albumins: a microcalorimetric investigation, Food Chem. 175 (2015) 137–142, http://dx.doi.org/10.1016/j.foodchem.2014.11.141.
[7] Q.T.H. Shubhra, J. Tóth, J. Gyenis, T. Feczkó, Surface modification of HSA containing magnetic PLGA nanoparticles by poloxamer to decrease plasma protein adsorption, Colloids Surf. B: Biointerfaces 122 (2014) 529–536, http://dx.doi.org/10.1016/j.colsurfb.2014.07.025.
[8] S.H. Lee, J.K. Suh, M. Li, Determination of bovine serum albumin by its enhancement effect of Nile blue fluorescence, Bull. Kor. Chem. Soc. 24 (2003) 45–48.
[9] C. Wang, Y. Zhou, K. Zhang, X. Nie, X. Xia, Fast and sensitive detection of protein concentration in mild environments, Talanta 135 (2015) 102–107, http://dx.doi.org/10.1016/j.talanta.2014.12.046.
[10] S.K. Kailasa, H. Wu, Functionalized quantum dots with dopamine dithiocarbamate as the matrix for the quantification of efavirenz in human plasma and as affinity probes for rapid identification of microwave tryptic digested proteins in MALDI-TOF-MS, J. Proteome 75 (2012) 2924–2933, http://dx.doi.org/10.1016/j.jprot.2011.12.008.
[11] Y. Ke, S.K. Kailasa, H. Wu, Z. Chen, High resolution detection of high mass proteins up to 80,000 Da via multifunctional CdS quantum dots in laser desorption/ionization mass spectrometry, Talanta 83 (2010) 178–184, http://dx.doi.org/10.1016/j.talanta.2010.09.003.
[12] S.K. Kailasa, H. Wu, Nanomaterial-based miniaturized extraction and preconcentration techniques coupled to matrix-assisted laser desorption/ionization mass spectrometry for assaying biomolecules, Trends Anal. Chem. 65 (2015) 54–72, http://dx.doi.org/10.1016/j.trac.2014.09.011.
[13] R.V. Hansen, M. Huang, Z. Zhan, G. Sun, J. Yang, L. Zheng, On the study of electrochromism in multiwalled carbon nanotube–polydiacetylene composites, Carbon N. Y. 90 (2015) 222–230, http://dx.doi.org/10.1016/j.carbon.2015.04.027.
[14] A.C.S. Pires, N. de F.F. Soares, L.H.M. da Silva, M. do C.H. da Silva, M.V. De Almeida, M. Le Hyaric, et al., A colorimetric biosensor for the detection of foodborne bacteria, Sensors Actuators B Chem. 153 (2011) 17–23, http://dx.doi.org/10.1016/j.snb.2010.09.069.
[15] S. Rozner, S. Kolusheva, Z. Cohen, W. Dowhan, J. Eichler, R. Jelinek, Detection and analysis of membrane interactions by a biomimetic colorimetric lipid/

polydiacetylene assay, Anal. Biochem. 319 (2003) 96–104, http://dx.doi.org/10.1016/S0003-2697(03)00278-1.
[16] L. Jiang, J. Luo, W. Dong, C. Wang, W. Jin, Y. Xia, et al., Development and evaluation of a polydiacetylene based biosensor for the detection of H5 influenza virus, J. Virol. Methods 219 (2015) 38–45, http://dx.doi.org/10.1016/j.jviromet.2015.03.013.
[17] A. Nopwinyuwong, T. Kitaoka, W. Boonsupthip, C. Pechyen, P. Suppakul, Effect of cationic surfactants on characteristics and colorimetric behavior of polydiacetylene/silica nanocomposite as time–temperature indicator, Appl. Surf. Sci. 314 (2014) 426–432, http://dx.doi.org/10.1016/j.apsusc.2014.07.013.
[18] A.C.S. Pires, N.F. Soares, L.H.M. Silva, M.C.H. SIlva, A.B. Mageste, F. Soares, et al., Thermodynamic study of colorimetric transitions in polydiacetylene vesicles induced by the solvent effect, J. Phys. Chem. B 114 (2010) 13365–13371, http://dx.doi.org/10.1021/jp105604t.
[19] R. Pimsen, A. Khumsri, S. Wacharasindhu, G. Tumcharern, M. Sukwattanasinitt, Colorimetric detection of dichlorvos using polydiacetylene vesicles with acetylcholinesterase and cationic surfactants, Biotechnol. Bioeng. 62 (2014) 8–12, http://dx.doi.org/10.1016/j.bios.2014.05.069.
[20] S. Lu, C. Jia, X. Duan, X. Zhang, F. Luo, Y. Han, et al., Polydiacetylene vesicles for hydrogen peroxide detection, Colloids Surfaces A Physicochem. Eng. Asp. 443 (2014) 488–491, http://dx.doi.org/10.1016/j.colsurfa.2013.11.029.
[21] T. Champaiboon, G. Tumcharern, A. Potisatityuenyong, S. Wacharasindhu, M. Sukwattanasinitt, A polydiacetylene multilayer film for naked eye detection of aromatic compounds, Sensors Actuators B Chem. 139 (2009) 532–537, http://dx.doi.org/10.1016/j.snb.2009.03.047.
[22] L. Tong, B. Cheng, Z. Liu, Y. Wang, Fabrication, structural characterization and sensing properties of polydiacetylene nanofibers templated from anodized aluminum oxide, Sensors Actuators B Chem. 155 (2011) 584–591, http://dx.doi.org/10.1016/j.snb.2011.01.014.
[23] T. Pattanatornchai, N. Charoenthai, S. Wacharasindhu, M. Sukwattanasinitt, R. Traiphol, Control over the color transition behavior of polydiacetylene vesicles using different alcohols, J. Colloid Interface Sci. 391 (2013) 45–53, http://dx.doi.org/10.1016/j.jcis.2012.10.004.
[24] J. Lee, J. Kim, Multiphasic sensory alginate particle having polydiacetylene liposome for selective and more sensitive Multitargeting detection, Chem. Mater. 24 (2012) 2817–2822, http://dx.doi.org/10.1021/cm3015012.
[25] M. Gou, G. Guo, J. Zhang, K. Men, J. Song, F. Luo, et al., Time–temperature chromatic sensor based on polydiacetylene (PDA) vesicle and amphiphilic copolymer, Sensors Actuators B Chem. 150 (2010) 406–411, http://dx.doi.org/10.1016/j.snb.2010.06.041.
[26] L.S. Virtuoso, M.D.S. Silva, B.S. Malaquias, K.A.S.F. Vello, P.R. Cindra, L. Henrique, et al., Equilibrium phase behavior of triblock copolymer + sodium or +potassium hydroxides + water two-phase systems at different temperatures, J. Chem. Eng. Data 55 (2010) 3847–3852, http://dx.doi.org/10.1021/je100335y.
[27] E.S. Lee, Y.T. Oh, Y.S. Youn, M. Nam, B. Park, J. Yun, et al., Binary mixing of micelles using Pluronics for a nano-sized drug delivery system, Colloids Surf. B: Biointerfaces 82 (2011) 190–195, http://dx.doi.org/10.1016/j.colsurfb.2010.08.033.
[28] A.M. Pragatheeswaran, S.B. Chen, Effect of chain length of PEO on the gelation and Micellization of the pluronic F127 copolymer aqueous system, Langmuir 29 (2013) 9694–9701, http://dx.doi.org/10.1021/la401639g.
[29] M.D. Charych, D.H. Nagy, J.O. Spevak, W. Bednarski, Direct colorimetric detection of a receptor-ligand interaction by a polymerized bilayer assembly, Science 261 (1993) 585–588, http://dx.doi.org/10.1126/science.8342021.
[30] A. Sahu, N. Kasoju, U. Bora, Fluorescence study of the curcumin-casein micelle complexation and its application as a drug nanocarrier to cancer cells, Biomacromolecules 9 (2008) 2905–2912, http://dx.doi.org/10.1021/bm800683f.
[31] L.C. De Souza, J. De Paula Rezende, A.C. Dos Santos Pires, L.H.M. Da Silva, M. do C.H. Da Silva, E.D.C. Castrillon, et al., Polydiacetylene/triblock copolymer nanoblend applied as a sensor for micellar casein: A thermodynamic approach, Food Chem. 197 (2016) 841–847, http://dx.doi.org/10.1016/j.foodchem.2015.11.071.
[32] J.M. Billakanti, C.J. Fee, F.R. Lane, A.S. Kash, R. Fredericks, Simultaneous, quantitative detection of five whey proteins in multiple samples by surface plasmon resonance, Int. Dairy J. 20 (2010) 96–105, http://dx.doi.org/10.1016/j.idairyj.2009.08.008.
[33] Y. Hang, L. Yang, Y. Qu, J. Hua, A new diketopyrrolopyrrole-based near-infrared (NIR) fluorescent biosensor for BSA detection and AIE-assisted bioimaging, Tetrahedron Lett. 55 (2014) 6998–7001, http://dx.doi.org/10.1016/j.tetlet.2014.10.108.
[34] R.W. Carpick, D.Y. Sasaki, M.S. Marcus, M.A. Eriksson, A.R. Burns, Polydiacetylene films: a review of recent investigations into chromogenic transitions and nanomechanical properties, J. Phys. Condens. MATTER. 16 (2004) 679–697, http://dx.doi.org/10.1088/0953-8984/16/23/R01.
[35] J. Causse, J. Oberdisse, J. Jestin, S. Lagerge, Small-angle neutron scattering study of solubilization of tributyl phosphate in aqueous solutions of L64 pluronic triblock copolymers, Langmuir 26 (2010) 15745–15753, http://dx.doi.org/10.1021/la1021164.
[36] D. Charbonneau, M. Beauregard, H.A. Tajmir-Riahi, Structural analysis of human serum albumin complexes with cationic lipids, J. Phys. Chem. B 113 (2009) 1777–1784, http://dx.doi.org/10.1021/jp8092012.
[37] S. Kolusheva, E. Wachtel, R. Jelinek, Biomimetic lipid/polymer colorimetric membranes: molecular and cooperative properties, J. Lipid Res. 44 (2003) 65–71, http://dx.doi.org/10.1194/jlr.M200136-JLR200.
[38] A.N. Bukiya, J.D. Belani, S. Rychnovsky, A.M. Dopico, Specificity of cholesterol and analogs to modulate BK channels points to direct sterol – channel protein interactions, J. Gen. Physiol. 137 (2011) 93–110, http://dx.doi.org/10.1085/jgp.201010519.
[39] P. Alexandridis, T.A. Hatton, Poly(ethylene oxide)-poly(propylene oxide)-poly (ethylene oxide) block copolymer surfactants in aqueous solutions and at interfaces: thermodynamics, structure, dynamics, and modeling, Colloids Surfaces A Physicochem. Eng. Asp. 7757 (1995) 1–46, http://dx.doi.org/10.1016/0927-7757(94)03028-X.
[40] S. Bhattacharya, S. Haldar, Interactions between cholesterol and lipids in bilayer membranes. Role of lipid headgroup and hydrocarbon chain-backbone linkage, Biochim. Biophys. Acta 1467 (2000) 39–53, http://dx.doi.org/10.1016/S0005-2736(00)00196-6.
[41] F. Meyer, B. Smit, Effect of cholesterol on the structure of a phospholipid bilayer, PNAS 106 (2009) 3654–3658, http://dx.doi.org/10.1073/pnas.0809959106.
[42] L. Rimnácová, P. Huseka, P. Simek, A new method for immediate derivatization of hydroxyl groups by fluoroalkyl chloroformates and its application for the determination of sterols and tocopherols in human serum and amniotic fluid by gas chromatography – mass spectrometry, J. Chromatogr. A. 1339 (2014) 154–167, http://dx.doi.org/10.1016/j.chroma.2014.03.007.
[43] K.S. Oh, H. Han, B.D. Yoon, M. Lee, H. Kim, D.W. Seo, et al., Effect of HIFU treatment on tumor targeting efficacy of docetaxel-loaded pluronic nanoparticles, Colloids Surf. B: Biointerfaces 119 (2014) 137–144, http://dx.doi.org/10.1016/j.colsurfb.2014.05.007.
[44] X. Fang, J. Zhang, X. Xie, D. Liu, C. He, J. Wan, et al., pH-sensitive micelles based on acid-labile pluronic F68 – curcumin conjugates for improved tumor intracellular drug delivery, Int. J. Pharm. 502 (2016) 28–37, http://dx.doi.org/10.1016/j.ijpharm.2016.01.029.
[45] M.H. Wang, J.H. Jeong, J.-C. Kim, Thermo-triggerable self-assembly comprising cinnamoyl polymeric β cyclodextrin and cinnamoyl pluronic F127, Colloids Surf. B: Biointerfaces 142 (2016) 148–158, http://dx.doi.org/10.1016/j.colsurfb.2016.02.048.
[46] S. Leavitt, E. Freire, Direct measurement of protein binding energetics by isothermal titration calorimetry, Curr. Opin. Struct. Biol. 11 (2001) 560–566, http://dx.doi.org/10.1016/S0959-440X(00)00248-7.
[47] A. Samanta, B.K. Paul, N. Guchhait, Novel proton transfer fluorescence probe 2-hydroxy-pyridine and 5-(4-fluorophenyl)-2-hydroxypyridine for studying native , denatured and renatured state of protein Bovine Serum Albumin, J. Photochem. Photobiol. B Biol. 101 (2010) 304–312, http://dx.doi.org/10.1016/j.jphotobiol.2010.07.016.
[48] I.M. Kuznetsova, B.Y. Zaslavsky, L. Breydo, K.K. Turoverov, V.N. Uversky, Beyond the excluded volume effects: mechanistic complexity of the crowded milieu, Molecules 20 (2015) 1377–1409, http://dx.doi.org/10.3390/molecules20011377.
[49] G. Zhang, Y. Ma, L. Wang, Y. Zhang, J. Zhou, Multispectroscopic studies on the interaction of maltol, a food additive, with bovine serum albumin, Food Chem. 133 (2012) 264–270, http://dx.doi.org/10.1016/j.foodchem.2012.01.014.
[50] R. Zeng, B.J. Bequette, B.T. Vinyard, D.D. Bannerman, Determination of milk and blood concentrations of lipopolysaccharide-binding protein in cows with naturally acquired subclinical and clinical mastitis, J. Dairy Sci. 92 (2009) 980–989, http://dx.doi.org/10.3168/jds.2008-1636.

Jaqueline de Paula Rezende is graduate student. She is studying in her Master the development of new sensor nanostrucutures to detect target molecules in food systems.

Guilherme Max Dias Ferreira received M.Sc. degree in 2012 in Agrochemistry. Currently he is a D.Sc. student and works with colloidal systems, isothermal microcalorimetry and fluorescence spectroscopy.

Gabriel Max Dias Ferreira received M.Sc. degree in 2012 in Agrochemistry. Currently he is a D.Sc. student and works with colloidal systems, isothermal microcalorimetry and fluorescence spectroscopy.

Luis Henrique Mendes da Silva obtained a D.Sc. degree in Chemistry in 2001. He holds na associate professor position in Chemistry Department of Federal University of Viçosa, Brazil. His main areas of interest are thermodynamic of colloidal systems and nanostructures, microcalorimetry, fluorescence and intermolecular interaction between chemical compounds.

Maria do Carmo Hepanhol da Silva received a D.Sc. degree in Chemistry in 1998. She is an associate professor in Chemistry Department of Federal University of Viçosa, Brazil. Her research covers analytical chemistry and spectroscopy techniques.

Maximiliano Soares Pinto holds a D.Sc. degree in Food Science and Technology in 2008. He is professor in Institute of Agriarian Science in Federal University of Minas Gerais, Brazil. His main area of interest is dairy science and technology.

Ana Clarissa dos Santos Pires obtained a D.Sc. degree in Food Science and Technology in 2009. She is professor in Food Technology Department of Federal University of Viçosa, Brazil. Her current research interest are development of new sensor nanostructures for detecting target molecules in food systems and intermolecular interaction between molecules present in food matrices.